Title

An experimental data base for the computational fluid dynamics of reacting and nonreacting methanol sprays

Journal

Journal of Fluids Engineering, Transactions of the ASME, 117(1)

ISSN

0098-2202

Authors

McDonell, VG
Samuelsen, GS

Publication Date

1995

DOI

10.1115/1.2816804

An Experimental Data Base for the Computational Fluid Dynamics of Reacting and Nonreacting Methanol Sprays

V. G. McDonell

G. S. Samuelsen

UCI Combustion Laboratory,
University of California,
Irvine, CA 92717-3550

The present data set consists of detailed measurements obtained within methanol sprays produced by a research atomizer which is operated with three atomizing air modes: none, non-swirling, and swirling. In addition, the cases with nonswirling and swirling atomizing air are characterized under reacting conditions. In each case, state-of-the-art diagnostics are applied. Measurements of the gas phase velocities in both the single and two-phase cases, droplet size distributions, and vapor concentration are obtained. The data are reported in a standardized format to ensure usefulness as modeling challenges. The results obtained reveal the presence of significant interaction between phases and significant changes in spray structure as a result of altering the atomizing air characteristics. Efforts have been directed toward delineation of errors and comparison with existing data sets where possible. The result is a comprehensive data base for vaporizing sprays under reacting and non-reacting conditions which permit a systematic variation in aerodynamic effects to be explored.

Introduction

In 1986, a NASA funded program for development of computational fluid dynamics codes for the prediction of complex aerothermochemical flows concluded that the development and verification of predictive codes was severely compromised by a lack of relevant and/or well documented experimental data (e.g., Mongia et al., 1986). One area in which data were found lacking is spray behavior. Recent developments in the area of spray characterization diagnostics are permitting information regarding spray behavior to be examined in great detail (e.g., McDonell and Samuelsen, 1990a). However, the goal of the majority of these studies has been to examine particular aspects of spray structure (e.g., droplet distribution means, droplet velocity). As a result of not measuring all aspects of the spray structure, these data sets have limited use for validation of computational fluid dynamic codes. Additionally, the majority of these data sets have *not* been made available in a format which provides the necessary information required for use in modeling challenges.

Recently, detailed data have been obtained in a series of evaporating sprays under both reacting as well as non-reacting conditions (McDonell and Samuelsen, 1993; McDonell et al., 1992; 1993a, b). These papers examine, in great detail, the structure of such sprays with the goal of providing insight not previously available. The present paper expands this data base and documents the results in a format (outlined in Appendix A) following that of Faeth and Samuelsen (1986).

The goal of the paper is to provide a collection of detailed data covering a range of fuel injector operation modes for model development, verification, and application.

Experiment

Fuel Injector. The fuel injector used for the present study is the Research Simplex Atomizer (RSA) which is manufactured by Parker Hannifin. Figure 1 presents details regarding the fuel injector geometry. A simplex injector tip is mounted centrally within a passage which allows air to be run through it. A swirler can be placed in the air passage to impart tangential momentum to the atomizing air. For the present data base, an additional concentric tube was placed over the end of the fixture shown to the left of Fig. 1, which brings the O.D. at the end of the inlet to 50.8 mm. Hence, the fuel injector assembly can be depicted as a round pipe 50.8 mm in diameter with a flat end and a hole 4.90 mm in diameter located at the center of the flat end.

The data base described features three modes of the injector operation: simplex (no atomizing air), nonswirling air-assist, swirling air-assist. The inlet geometry modifications required to obtain these modes are depicted in Fig. 2. In each case, the external geometry of the fuel injector remains the same. Hence, the only change made from a CFD standpoint is a modest change in inlet conditions.

Fuel. Methanol is employed for the testing. It is a single component fuel, so effects of variation in volatility with fuel

Contributed by the Fluids Engineering Division for publication in the JOURNAL OF FLUIDS ENGINEERING. Manuscript received by the Fluids Engineering Division May 6, 1993; revised manuscript received April 27, 1994. Associate Technical Editor: A. Prosperetti.

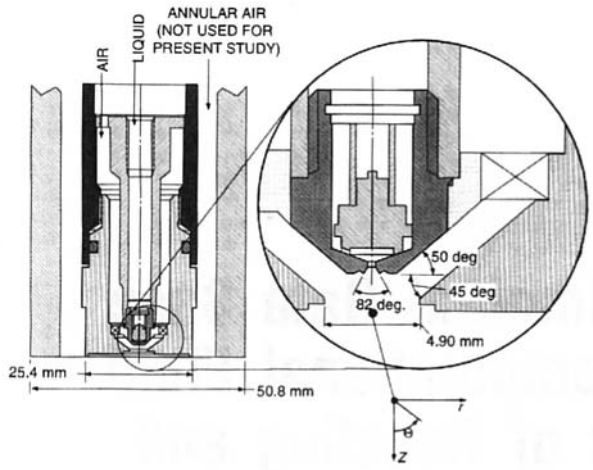

Fig. 1 Research simplex atomizer

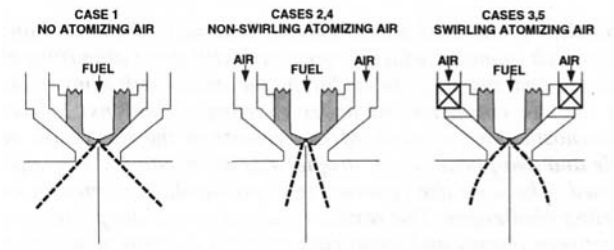

Fig. 2 Three modes of injection

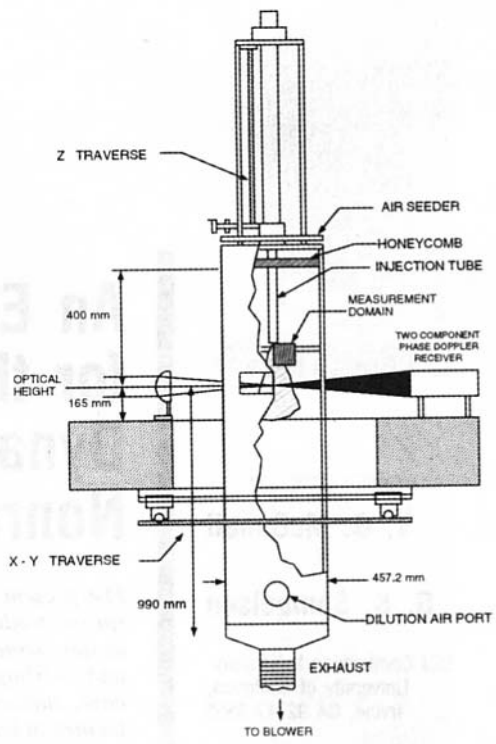

Fig. 3 Schematic of facility and measurement domain

composition are removed. For non-reacting conditions, the density of the methanol vapor is similar to that of air. Finally, for reacting conditions, the flame is relatively soot free which is attractive for characterization with non-intrusive diagnostics. As described below, the use of methanol also helps to reduce systematic errors associated with the optical diagnostic used.

Operating Conditions. The five cases included in the data base utilize methanol injected at a mass flow rate of 1.26 g/s (420 kPa pressure drop). When air is utilized (Cases 2–5), a mass flow rate of 1.32 g/s is injected. For the cases without swirl, this air flow results in a pressure drop of 3.73 and 3.48 kPa for conditions with and without spray, respectively. For cases with swirling atomizing air (Cases 3 and 5), the pressure drop is 13.79 kPa. Methanol and air are injected at 18–22 C.

Boundary Conditions. In each case, the sprays injected downwards from the center of a 495 × 495 mm square duct. Air is pulled through the top of the duct by a blower at a bulk velocity of 0.8 m/s. Measurements away from the centerline revealed that sufficient air is injected to enable a zero gradient boundary condition to be imposed near the wall of the duct (approximately 180 mm from the centerline). Measurements are obtained at axial locations, Z, of 15, 25, 35, 50, 75, 100, and 150 mm downstream of the injector. In addition, an "inlet" plane measurement is obtained near the injector. For the sprays considered, physical constraints (i.e., nonspherical drops) for the PDI permitted measurements to be obtained 7.5 mm downstream. For each case, this is taken as the "inlet" boundary. Figure 3 illustrates the overall geometry and indicates the relation of the measurement domain to the flow field.

Diagnostics. Phase Doppler-Interferometry (PDI) is the primary diagnostic tool employed. Additional details regarding the instrument as utilized for the present study are available elsewhere (McDonell and Samuelsen, 1990b, McDonell and Samuelsen, 1993). Note that the PDI system is used to measure the gas phase velocities in the presence of the spray. This is achieved by seeding all the air streams, optimizing the instrument to detect small particles, and then, via post-processing, isolating the velocity statistics associated with the small particles.

The vapor concentration measurement system (IRES) is also described in detail elsewhere (Adachi et al., 1991).

Results and Discussion

Global Structure. Figure 4 presents photographs of the five cases (Figs. 4 (a–e) correspond to Cases 1–5, respectively). The first three photos document the nonreacting sprays (Figs. 4(a–c)) and reveal the impact of the operating mode on the overall spray structure. The addition of non-swirling atomizing air collapses the spray and results in an apparent increase in concentration. Adding swirl to the air-assist results in a broadening of the spray compared to the case without swirl as well as an increase in the structure at the outer edges.

The reacting cases (Figs. 4(d–e)) reveal that the droplets are rapidly consumed downstream of the atomizer. In both cases, droplets at the centerline persist the farthest downstream. Note also that packets of isolated droplets appear in regions away from the centerline.

Gas Phase Behavior. To provide an overview of the gas phase behavior in the presence of the spray, Fig. 5 presents vectors of the velocity in the r-Z plane along with contours which depict the mean hydrocarbon concentration. Note that, in each non-reacting case, measurements of the single phase flow (absence of spray) are also available. These results are not included in detail here for brevity, but provide cases which eliminate, as a first step, the complexities of the two-phase interaction.

Figures 5(a–c) present results for the nonreacting cases. The gas phase velocities are strongly dependent upon the presence of atomizing air, as expected. In the case without atomizing air (Case 1: Fig. 5(a)), the gas phase mean velocities are generally less than 5 m/s. The results reveal the presence of entrainment associated with the injection of the spray. As the air

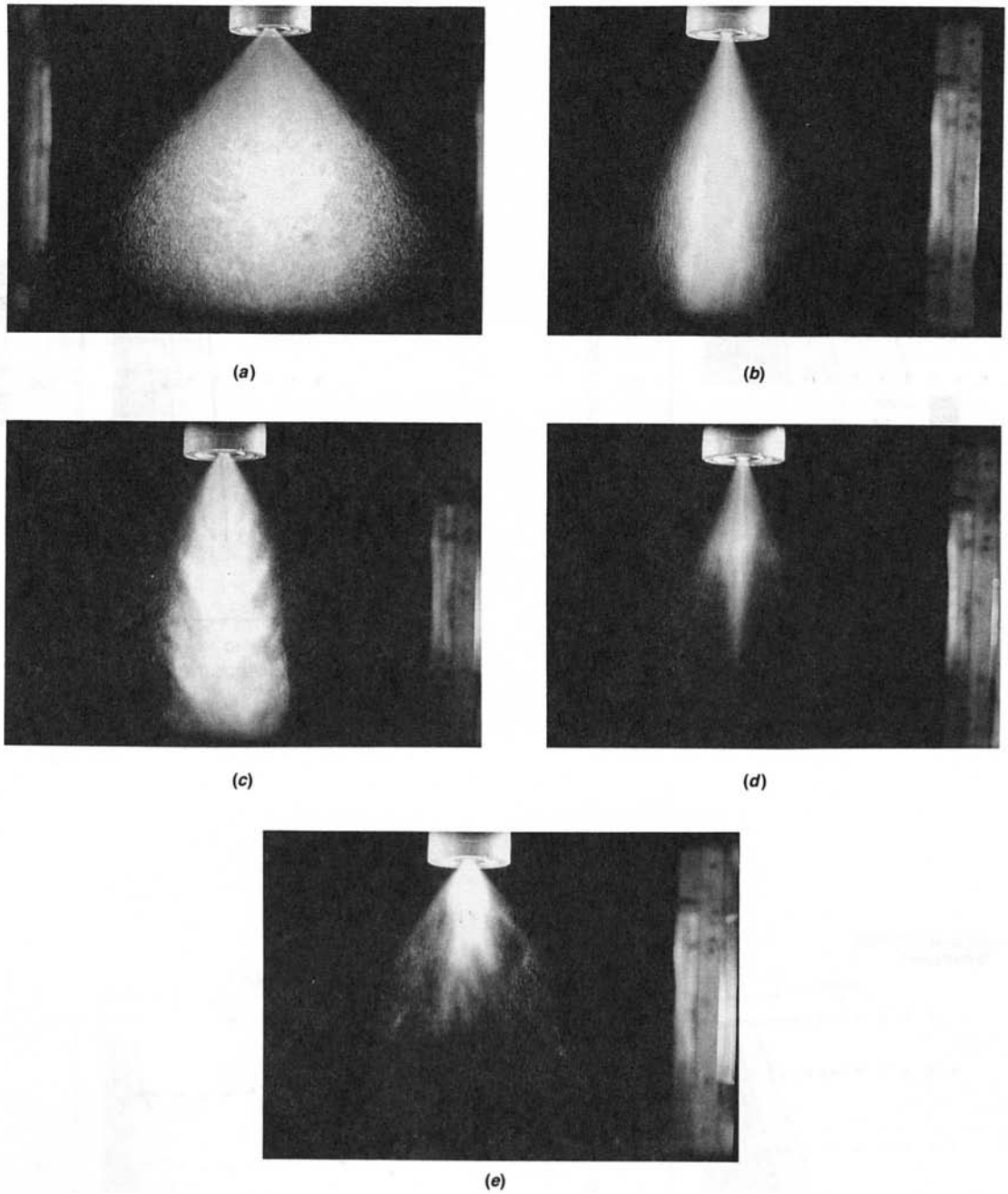

Fig. 4 Backlit photographs of the sprays for the five cases Fig. 4(*a*) Case 1 Fig. 4(*b*) Case 2 Fig. 4(*c*) Case 3 Fig. 4(*d*) Case 4 Fig. 4(*e*) Case 5

entrained reaches the area near the spray, it is accelerated by the spray and moves away from the centerline. By 75 mm downstream, the momentum exchange between phases is nearly completed and the gas moves nearly straight down. Note that, at regions away from the centerline, the air flow is essentially flowing in the axial direction.

The vapor concentration contours reflect, to a degree, the locations where the spray exists. The maximum concentrations exist at the centerline (3.8 percent by volume). This is attributed to (1) the presence of large numbers (McDonell and Samuelsen, 1990b) of small droplets in this region moving at low velocities (i.e., short vaporization time combined with long residence time) and (2) low dilution associated with entrainment air from outside the spray. Based on calculations and psychrometer experiments, the saturation temperature for methanol under the experimental conditions considered is between −8 and −4°C. If 3.8 percent vapor concentration is assumed to be a saturated condition, the gas temperature would be −3.7 to −1°C, suggesting that the conditions at the centerline of the CASE 1 spray are nearly saturated, precluding additional vaporization in this region. The vapor concentrations decrease with increased distance from the centerline due to entrainment of air surrounding the spray and a decrease in the total droplet concentration.

When non-swirling air-assist is added (Case 2: Fig. 5(*b*)), several changes in the Case 1 velocities are apparent. The velocities at the centerline are greatly enhanced (reaching 50 m/s). The spray width is reduced (Fig. 4(*a*)) which results in strong interaction with the gas phase in regions nearer to the centerline.

Like the Case 1 spray, the vapor concentrations in the Case 2 spray are highest at the centerline (2.4 percent). For Case 2, however, two sources of dilution exist, entrainment from the surrounding air and the atomizing air itself. As a result,

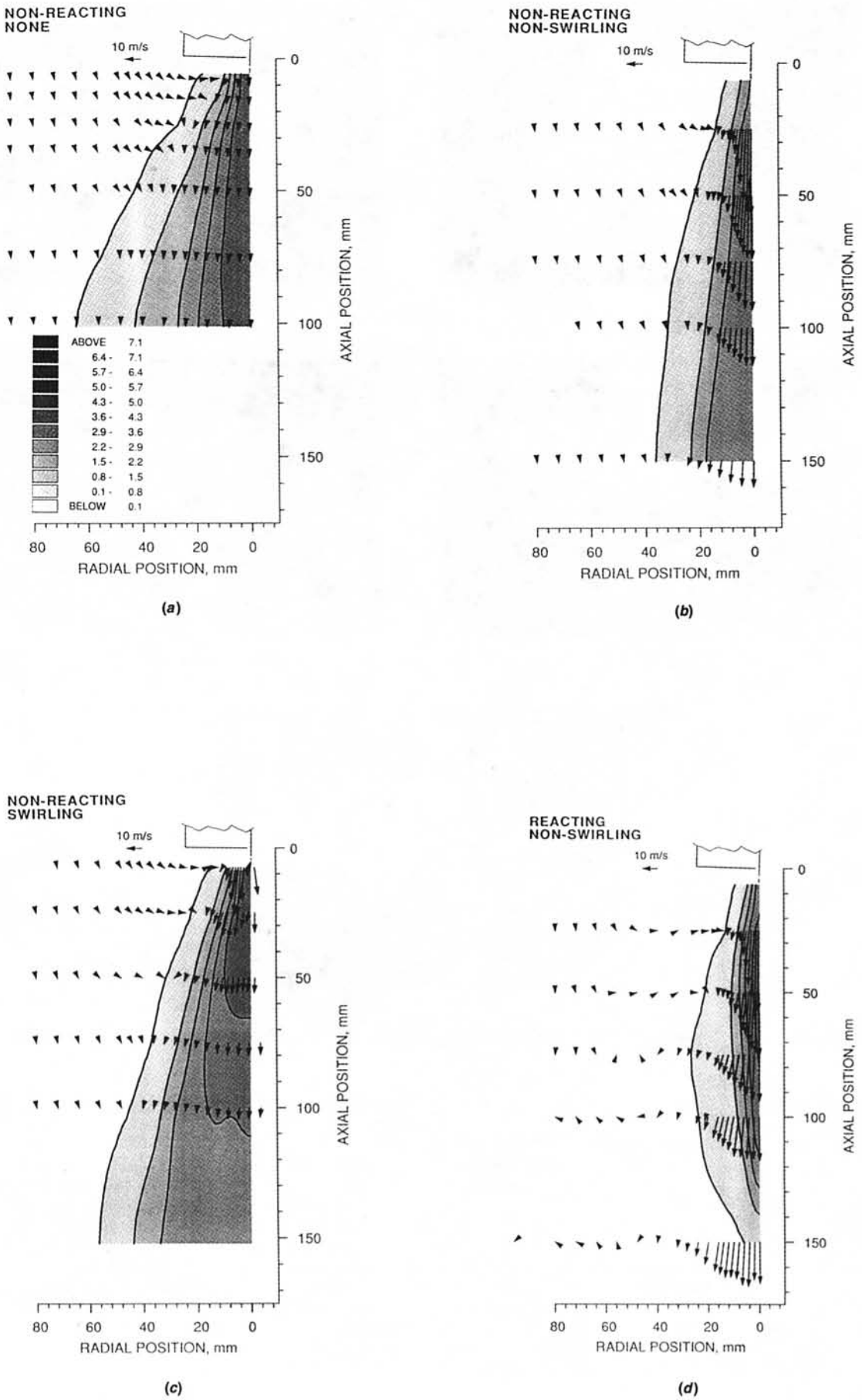

Fig. 5 Gas phase vectors in the *r-Z* plane and contours of hydrocarbon vapor percent by volume Fig. 5(*a*) Case 1 Fig. 5(*b*) Case 2 Fig. 5(*c*) Case 3 Fig. 5(*d*) Case 4 Fig. 5(*e*) Case 5

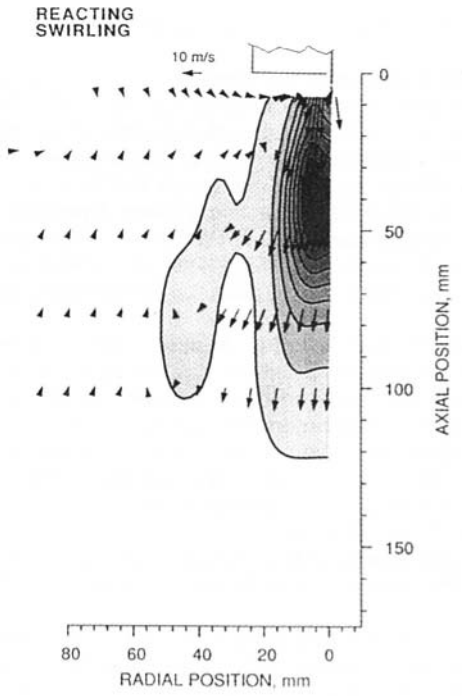

(e)

Fig. 5 Continued

the Case 2 spray may not be expected to reach saturation. However, convective effects may lower the temperature within the spray, resulting in lower concentrations at the saturated condition. Away from the centerline, entrainment of the surrounding air becomes significant enough to lower the vapor concentration.

When swirl is added to the atomizing air (Case 3: Fig. 5(*c*)), several features in the velocity change. In this case, a small recirculation zone is formed immediately downstream of the injector. This results in a local minimum in velocity at the centerline with increased distance from the injector. Compared to the Case 2 spray, an increase in the width is apparent (consistent with Figure 4a). The swirl reduces the maximum axial velocities.

The vapor concentrations in the Case 3 spray feature a local maximum at the centerline within a region extending about 65 mm downstream. The maximum concentrations in this region (3.6 percent) approach those in the Case 1 spray. In this case, the velocities are lower (increased residence time, decreased convective transfer), hence a saturation condition is more likely than in the Case 2 spray.

Figures 5(*d–e*) presents the same results for the reacting cases (Cases 4 and 5). The reacting case with nonswirling atomizing air (Fig. 5(*d*)) reveals features which are similar to those for the non-reacting case. The axial velocities retain the maximum values at the centerline. With increased distance downstream, the velocities increase compared to the non-reacting case due to the expansion of the gases. Note that, in the flow away from the spray, a region of reverse flow is present. This is due to buoyancy effects (recall that the experiment is downfired). In the Case 4 spray, this external recirculation zone helps to stabilize the reaction.

The vapor concentrations in the Case 4 spray still show a maximum at the centerline. In this case, the vapor is consumed as well as produced, so what is presented is really unburned hydrocarbons. The peak levels for the Case 4 spray (3.6 percent) suggest a lean reaction.

The velocities and vapor concentrations in reacting case with swirling atomizing air (Case 5: Fig. 5(*e*)) reflect the general

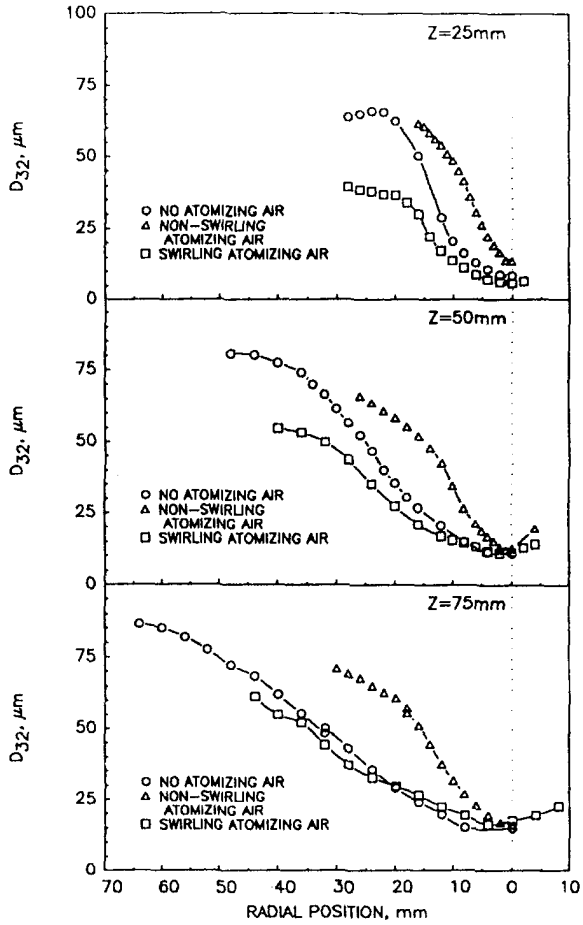

Fig. 6 Comparison of droplet size distribution sauter mean diameter for the nonreacting sprays

trends of the corresponding nonreacting case (3). Like Case 4, an external recirculation zone is formed which is due to buoyancy. In this case, more droplets are present in the region away from the centerline (recall Fig. 3(*b*)), and these droplets (local vapor sources) combined with the external recirculation zone lead to the "peninsula" of vapor away from the centerline.

Droplet Behavior. Figures 6 and 7 present comparisons of the droplet mean behavior in the non-reacting cases at three axial locations. Figure 6 compares the droplet size distribution Sauter mean diameter. In the absence of atomizing air, the radial profiles are typical of those from a hollow cone simplex spray, namely: minimum values at the centerline and maximum values at some radial location. This is due to isolation of drops according to momentum. Initially, the fuel is injected in an cone-annular sheet which, in this case, has an angle of 89 deg. As the sheet breaks up, small drops shed off both sides, with the larger drops maintaining a trajectory which is close to that of the original sheet. As the spray moves downstream, air entrained from the surroundings imparts a force radially inwards on the drops. This force results in more motion for small drops, and they are carried in towards the centerline. At axial locations close to the injector, the shedding of small drops off the outer and inner surface of the sheet leads to a local maximum in drop size at some radial distance from the centerline with smaller sizes found at radial locations beyond this distance. This effect disappears with increasing axial distance because the small drops on the outside of the sheet are carried back inside the trajectory of large drops.

When nonswirling atomizing air is added, the effect is primarily a collapse of the spray with only a small effect of the drop size. A concise statement of the droplet mean size is a

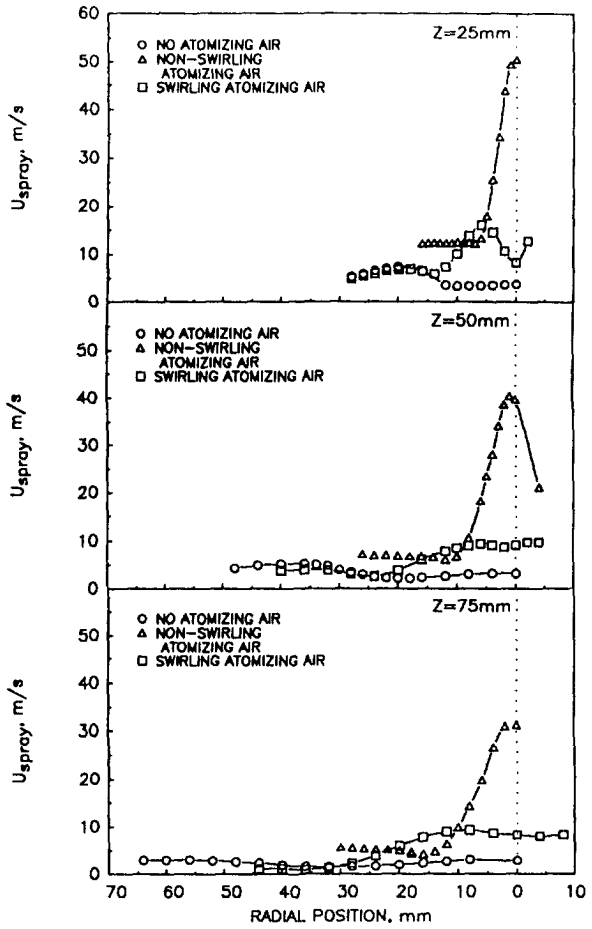

Fig. 7 Comparison of droplet mean axial velocity for the nonreacting sprays

line-averaged Sauter mean diameter. Using this as a quick indication of trends in drop size, at an axial location of 75 mm, the average drop size decreases from 35.3 μm to 31.5 μm when non-swirling atomizing air is added. This is somewhat surprising since the atomizing air impacts the cone-annular sheet at nearly normal angles. When swirl is added, the spray width is increased, and the average drop size is significantly reduced (from 31.5 μm to 17.4 μm).

Figure 7 presents the impact of the injection mode on the spray mean axial velocity. Note that this is the number weighted mean axial velocity for the entire spray. It does not account for size-velocity correlations. The trends in the droplet velocity are similar to those for the gas phase. The drop velocities for the spray with no atomizing air are generally less than 10 m/s. When non-swirling atomizing air is added, the droplet velocities are increased dramatically. Adding swirl to the atomizing air results in a reduction of this velocity, but to levels which are still greater than those found in the case without atomizing air.

These same types of results are available for the reacting cases as well (McDonell and Samuelsen, 1990b). Reaction does not change the general trends observed in the comparisons shown in Figs. 6 and 7. The primary effect of the reaction is to reduce the droplet size distribution means. However, it is also observed that the span of the distribution tends to increase with the presence of reaction. Also, the mean velocity measured at a given point increases. The interpretation of the drop velocity is challenging in the reacting case because the drop size is continually changing. This makes discrimination between momentum transfer between phases nearly impossible. In fact, a suitable predictive code could fill in the needed insight to better understand the role of vaporization and momentum transfer.

In order to determine the behavior of a particular size class, the mean velocity statistics can be calculated as a function of size class. Figure 8 presents radial profiles of the mean axial velocity as a function of droplet size for the non-reacting cases. The left column presents these results for the case without atomizing air (Case 01). Note that a strong dependency of drop velocity on drop size exists. For reference, the gas phase mean axial velocity is included. Significant slip velocities exist, indicating that strong momentum transfer between phases is occurring.

The middle portion of Fig. 8 presents the same type of results for the case with non-swirling atomizing air (Case 02). The trends are similar to those observed in the case without atomizing air. The primary differences are that the magnitude of the velocities are higher and, near the centerline, the velocity of gas phase exceeds that of the drops. This results in a situation where, at the centerline, momentum is transferred from the drops to the gas.

The right column of Fig. 8 presents the results for the case with swirling atomizing air (Case 03). Similar trends are observed.

Once again, the companion results for the reacting case are not presented for brevity, but are available as part of the data base (McDonell and Samuelsen, 1990b).

Quality Assurance Efforts. A primary challenge in applying state-of-the-art diagnostics to complex systems is the ensuring of accuracy. In the present data base, efforts were made, where possible, to ensure the quality and accuracy of the results. The following section delineates examples of the actions taken to ensure data quality.

Absolute Comparisons. Each instrument is subject to systematic errors associated with noise, optical alignment, etc. In the present data base, specific tests were carried out to better understand the fundamental limits in the measurement accuracy. The PDI instrument absolute accuracy suffers additionally from being dependent upon the spray measured. To this end, two studies were conducted in support of this data base as well as for general applications of the PDI instrument (McDonell and Samuelsen, 1990c; McDonell and Samuelsen, 1991). No short answer exists for determining the accuracy of the PDI measurements. The studies do indicate that the size and velocity of a single droplet can be measured with good accuracy (3 percent error in size, 1 percent error in velocity). Where the significant shortcomings arise are in the absolute counting of particles and the representation of the polydispersion. PDI is a single particle counter. If more than one particle enters the probe volume, either one or both particles will be invalidated (and hence quantities such as volume flux and concentration are subject to the largest errors). In addition, the dependency of the sample volume upon particle size must be somehow accounted for. The algorithms utilized suffer from inaccuracies and assumptions. As a result, the accuracy must be inferred from other tests (e.g., comparisons to other instruments, mass flux profile integrations).

The IRES measurement accuracy was evaluated for the sprays measured for the data base and are documented in Adachi et al., 1991. For the system used for in the present data base, the detectability limit is 0.1 percent. Maximum systematic errors of 7 percent and 15 percent are assigned to the nonreacting and reacting data, respectively.

A check which is often conducted for PDI measurements involves integration of a radial profile of volume flux. This integration should lead to the total liquid flow rate through the axial plane where measurements were obtained. In a vaporizing spray, some value which is less than the metered flow to the injector should be obtained. However, in the absence of quantification of the vaporization, this cannot give an ab-

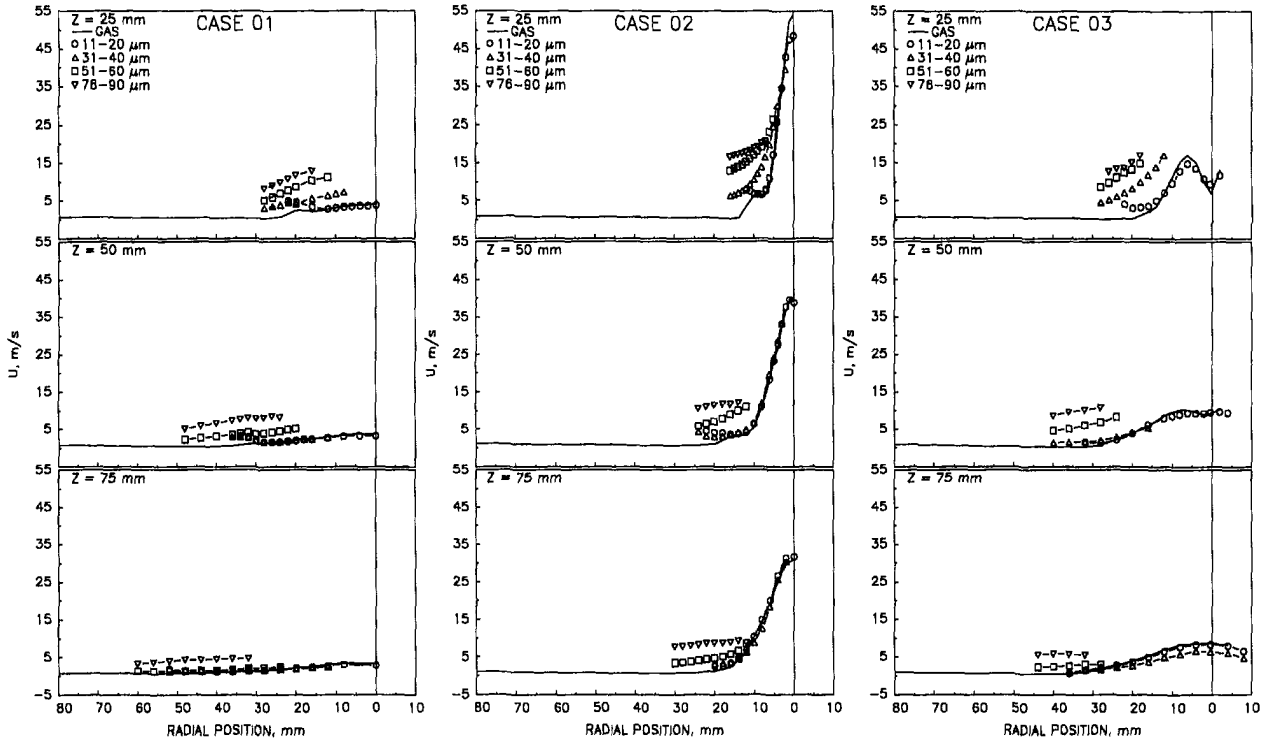

Fig. 8 Correlation between drop size and velocity for the nonreacting sprays

Table 1 Mass conservation in the nonreacting sprays

Case	Axial Plane	Liquid flow via PDI (g/s)[a]	Vapor flow via IRES (g/s)[b]	Total (g/s)	% Mass total[c]
1	25	0.914 ± 0.171	0.073 ± 0.007	0.987	78 ± 14
	75	1.130 ± 0.317	0.200 ± 0.020	1.330	106 ± 27
2	25	0.407 ± 0.048	0.075 ± 0.007	0.482	38 ± 5
	75	0.587 ± 0.226	0.185 ± 0.019	0.772	61 ± 19
3	25	0.299 ± 0.084	0.251 ± 0.025	0.550	44 ± 9
	75	0.434 ± 0.168	0.397 ± 0.056	0.831	66 ± 18

[a]Errors are established in this case by utilizing the ratio of samples attempted to samples validated at each radial location. The metered injected liquid mass flow rate is 1.26 g/s.
[b]A maximum systematic error of 7% was established for these sprays. Symmetry effects generally resulted in an additional 3% in uncertainty. At 75 mm for Case 3, asymmetries in the gas velocity (needed to compute vapor flux) are reflected as well.
[c]Assumes that errors in PDI and IRES are summed linearly and should reflect a "worst case" scenario.

solute comparison. In the present case, the IRES measurements can be combined with the PDI measurement of gas phase velocity to provide the total flow rate of vapor through each plane (McDonell and Samuelsen, 1992). The measurement of liquid flow (PDI) and vapor flow (IRES) permits accountability of all methanol injected. Table 1 summarizes these quantities at an axial locations of 25 and 75 mm.

At least two points are illustrated in Table 1: (1) mass conservation is worse at locations close to the injector, and (2) significant errors exist in the figures. In the cases where significant mass is not accounted for, yet errors are small (e.g., Case 3, Z = 25 mm), it is likely that many multi-drop occurrences are detected. Although initially disconcerting, the lack of mass conservation due to high concentrations does not likely invalidate distribution averages (Edwards and Marx, 1992). What is compromised in these cases are the measurement of total drop population (i.e., concentration), and volume flux. This must be considered when utilizing the present data for model comparison.

Symmetry Evaluation. For Cases 1 and 2, detailed symmetry assessments were carried out. This was accomplished by making PDI measurements for different injector orientations (in 45 deg increments). An example of the symmetry for the Case 2 spray is shown in Fig. 9. The results shown are the mean value from a given radial location with error bars which reflect the standard deviation about the mean. The Case 2 spray reveals excellent symmetry in terms of both gas phase velocities as well and distribution means. Case 1 shows similar

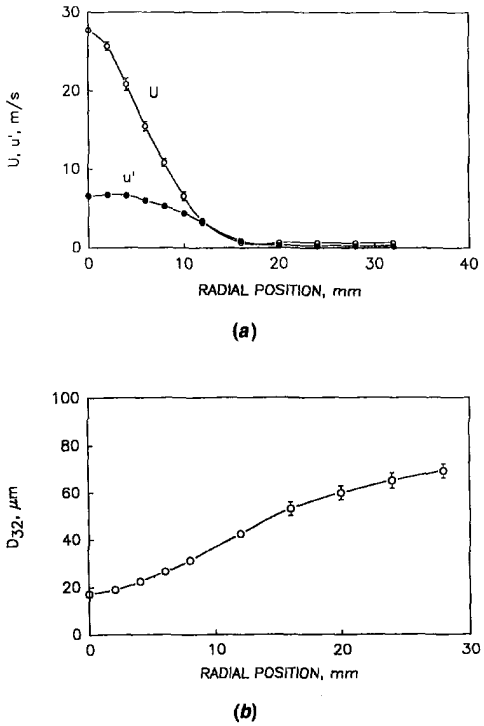

Fig. 9 Symmetry of the Case 2 spray

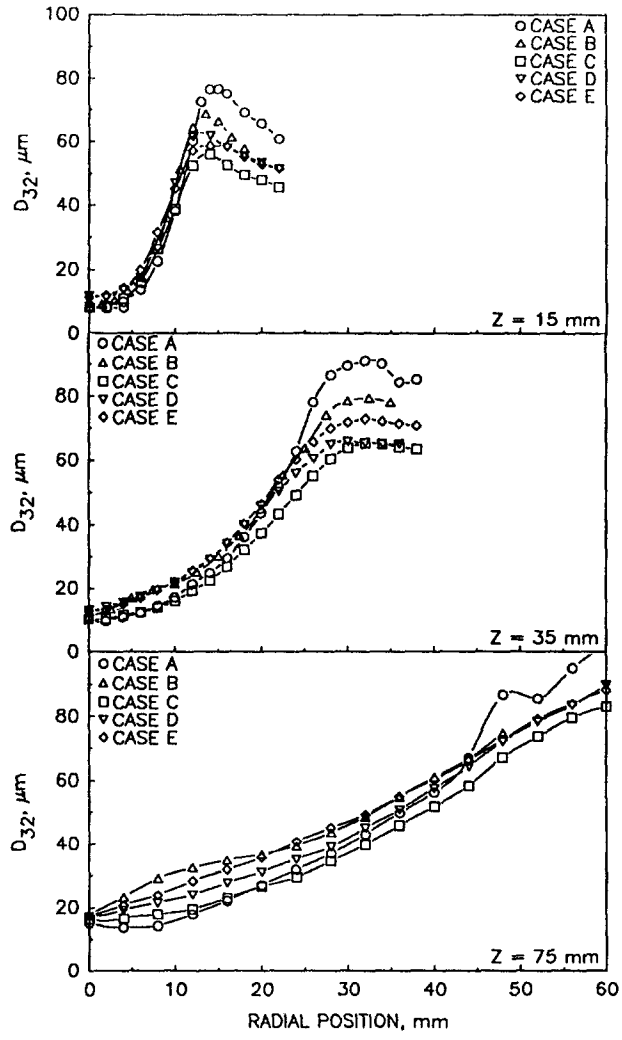

Fig. 10 Example of interlaboratory comparison for Case 1 spray (McDonell et al., 1994)

symmetry. The symmetry for Case 3 is not as good as for Case 1 and 2.

Repeatability. For Cases 1–3, at least two sets of PDI data were obtained. Generally, the mean quantities measured at a given point repeated to within 5 percent. In order to provide a more meaningful case for repeatability, the Case 1 spray has been characterized as part of an interlaboratory comparison (McDonell et al., 1994). Figure 10 presents an example of the comparison. In this study, five data sets (Cases A–E in Fig. 10) were obtained over a 27 month period of time on the same injector. The results show the degree to which measurements obtained in independent laboratories repeat.

Comparison to Existing Data. Unfortunately, spray characterization results are highly system specific. It is uncertain what level of agreement should be expected between detailed measurements obtained in general systems. In the current data base, some examples are available for the Case 1 spray where direct comparison can be made with existing data. In addition to the interlaboratory test carried out (McDonell et al., 1994), results previously obtained were also available (Dodge, 1986). An example of the comparison of the results from the present spray is shown in Fig. 11.

Summary and Conclusions

Detailed and well documented data sets, following the format prescribed in Appendix A, are available for the development and verification of computation codes proposed for spray behavior (McDonell and Samuelsen, 1990b). The data sets reveal that changes in the injection mode has profound effects on the spray behavior. In addition, the results provide cases in which momentum transfer occurs both to and from the droplets. Finally, the inclusion of vapor measurements within the sprays allows, for the first time, both diffusion and thermal gradient driven vaporization models to be evaluated.

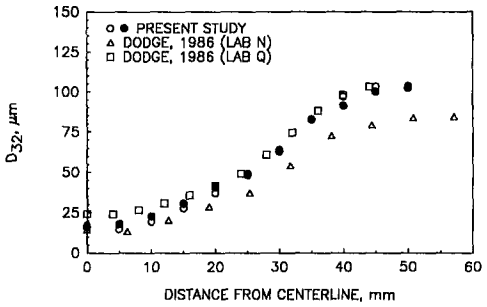

Fig. 11 Comparison of Case 1 spray measurements to data of Dodge (1986)

Acknowledgment

The continued support of Parker Hannifin for studies in the area of spray characterization is greatly appreciated.

References

Adachi, M., McDonell, V. G., and Samuelsen, G. S., 1991, "Non-Intrusive Measurement of Gaseous Species in Reacting and Non-Reacting Sprays," *Combustion Science and Technology*, Vol. 75, pp. 179–194.

Edwards, C. F. and Marx, K. D., 1992. "Analysis of the Ideal Phase-Doppler System: Limitations Imposed by the Single-Particle Constraint," *Atomization Sprays*, Vol. 2, pp. 319–366.

Dodge, L. G., 1986, "Comparison of Drop-Size Measurements for Similar Atomizer," Special Report, SwRI-8858/2, Southwest Research Institute, San Antonio, TX.

Faeth, G. M. and Samuelsen, G. S., 1986, "Fast-Reaction Nonpremixed Combustion," *Progress in Energy and Combustion Science*, Vol. 12, No. 4, pp. 305–372.

McDonell, V. G. and Samuelsen, G. S., 1990a, "Application of Laser Interferometry to the Study of Droplet/Gas Phase Interaction and Behavior in Liquid Spray Combustion Systems," *Combustion Science and Technology*, Vol. 74, pp. 343–359.

McDonell, V. G. and Samuelsen, G. S., 1990b, "Detailed Data Set: PDI and IRES Measurements in Methanol Sprays Under Reacting and Non-Reacting Conditions, Case A–C," UCI Combustion Laboratory Report UCI-ARTR-90-17A-C.

McDonell, V. G. and Samuelsen, G. S., 1990c, "Sensitivity Assessment of a Phase-Doppler Interferometer to User-Controlled Settings," *Liquid Particle Size Measurement Techniques: 2nd Volume, ASTM STP 1083*, E. Dan Hirleman, W. D. Bachalo, and Philip G. Felton, eds., ASTM, Philadelphia, pp. 170–189.

McDonell, V. G. and Samuelsen, G. S., 1991, Data Quality Control Evaluation of the Aerometrics Two-Component Phase Doppler Interferometer. UCI Combustion Laboratory Report UCI-ARTR-91-1.

McDonell, V. G. and Samuelsen, G. S., 1992, "Effect of Fuel Injection Mode on Fuel Vapor in Reacting and Non-Reacting Methanol Sprays," *24th Symposium (International) on Combustion*, The Combustion Institute, Pittsburgh, PA, pp. 1557–1564.

McDonell, V. G. and Samuelsen, G. S., 1993, "Structure of Vaporizing Pressure Atomized Sprays," *Atomization and Sprays*. Vol. 3, No. 3, pp. 321–364.

McDonell, V. G., Adachi, M., and Samuelsen, G. S., 1992, "Structure of Reacting and Non-Reacting Swirling Air-Assisted Sprays," *Combustion Science and Technology*, Vol. 82, pp. 225–248.

McDonell, V. G., Adachi, M., and Samuelsen, G. S., 1993a, "Structure of Reacting and Non-Reacting Non-Swirling Air-Assisted Sprays, Part I: Gas Phase Properties," *Atomization and Sprays*, Vol. 3, No. 4, pp. 389–410.

McDonell, V. G., Adachi, M., and Samuelsen, G. S., 1993b, "Structure of Reacting and Non-Reacting Non-Swirling Air-Assisted Sprays, Part II: Droplet Behavior," *Atomization and Sprays*, Vol. 3, No. 4, pp. 411–436.

McDonell, V. G., Samuelsen, G. S., Wang, M. R., Hong, C. H., and Lai, W. H., 1994, "Interlaboratory Comparison of Phase Doppler Measurements in a Research Simplex Atomizer Spray," *AIAA J. Propulsion and Power*, Vol. 10, No. 3, pp. 402–409.

Mongia, H. C., Reynolds, R. S., and Srinivasan, R., 1986, "Multidimensional Gas Turbine Combustor Modeling: Applications and Limitations," *AIAA Journal*, Vol. 24, No. 6, pp. 890–904.

APPENDIX A

Recommended Format for Data Base Documentation (Faeth and Samuelsen, 1986)

1 Experimental Facility
2 Experimental Configurations
3 Test Conditions
4 Inlet and Boundary Conditions
5 Quantities Measured
6 Diagnostics
7 Unusual Measurement Methods
8 Experimental Protocol
9 Quality Control
10 Error Analysis
11 Availability of the Data
12 References
13 Data